

# Dynamic Characteristics for the Iconic Tower According to the Egyptian Code

Khaled Muhammad Ali Muhammad<sup>1</sup>, Amin Saleh Aly<sup>2</sup>, Ahmed Elsayed Awwad Hassanein Elsafty<sup>3</sup>

<sup>1</sup>Civil Engineering Department, Pyramids Higher Institute for Engineering and Technology, Cairo, Egypt

<sup>2</sup>Civil Engineering Department, Ain Shams University, Cairo, Egypt

<sup>3</sup>Civil Engineering Department, Ain Shams University, Cairo, Egypt

**Abstract:** A new generation of design and rehabilitation procedures that incorporate performance-based engineering concepts must be developed. These include assessing the structural strength and available capacities and contrasting them with the deformation requirements associated with acceptable performance levels. This study examines the performance of outrigger system under seismic hazards using the structural non-linear static analysis procedure (NSP). The post-yield behavior, relative damage of the structure, story shears, roof displacement, story drifts, story moments, time period, structure performance level, and response modification factor (R) of the Iconic Tower were all assessed using response spectrum analysis (RSA) and pushover analysis (POA). Moreover, this study sheds light on the structural system of The Iconic Tower for attempting to calculate the seismic response coefficient (R-Reduction Factor) also the natural frequency of the structure by the Egyptian code through an analytical study in the context of keeping up with recent developments in the field of high-rise buildings.

**Keywords:** Dynamic analysis, dynamic characteristics, natural frequency, outrigger system, response modification factor, r-factor

## 1. Introduction

The designs criteria for wind and earthquake loads differ from those for gravity (dead and living) loads. Wind loads are a major necessity since loading situations occur frequently. In high-seismic areas, structures are designed to withstand lateral movements as well. Structures are generally built to handle lateral wind loads that constitute roughly 1% to 3% of their entire weight. However, if the same elastic design concepts were applied, earthquake loads may reach 30–40% of the structure's weight, which could lead to incredibly heavy and costly constructions. As a result, the R-factor's significance becomes evident when earthquake design incorporates the ideas of controlled damage and collapse avoidance.

One important factor in the design of seismic building is the response modification factor (R). Determining R makes it probable to do equivalent statistical analysis, which is widely used to determine the seismic response of buildings. Specifically, R denotes a structure's capacity to distribute energy via inelastic behavior, as demonstrated by current building rules. Researchers Wu et al., 1989; Hanson et al., 1993; Federal Emergency Management Agency (FEMA)-273, 1997; National Earthquake damages Reduction Program (NEHRP), 1994; and other researchers largely concentrated on displacement response when examining the impact of R. The Uniform Building Code (UBC, 1994) and NEHRP (1994) both used Wu et al. (1989) findings to develop passive energy dissipation systems. The International Building Code (IBC, 2000), UBC (1997), FEMA-273 (1997), NEHRP-97 (1997), Applied Technology Council (ATC)-40 (1996), and Structural Engineers Association of California (SEAOC) Blue Book (1999) all used the ideas of Newmark and Hall (1982) to design buildings with passive energy dissipation and seismic isolation systems. Current seismic design codes, such the NEHRP and UBC codes, rely on force-based methods. On

other side, the effect of viscous damping on the displacement response of elastic single-degree-of-freedom (SDOF) systems are the source of damping reduction factors that are allowed in codes. ATC-19 (1995) and other documents calculate the impacts of additional dampening to reduce a building's force response. It is anticipated that adding more damping to a building will lessen displacements. In the US, the fundamental approach for seismic design is still static elastic analysis. For more than 70 years, the static lateral force method has been applied in various ways (ATC, 1995b). In order to decrease base shear force ( $V_e$ ), which is determined using elastic analysis of the 5% damped acceleration response spectrum ( $S_{a,5}$ ), and to measure design base shear force ( $V_b$ ), ATC-3-06 (1978) established R in the late 1970s. The SEAOC Blue Book (1999) and ATC (1995a) allow empirical horizontal force factors for determining the R value, which can range from two to eight ductile seismic framing systems.

IBC (2000) states that the deflection amplification factor ( $C_d$ ) and the design of reduced seismic forces of structures to transform elastic lateral displacements into total lateral displacements should be evaluated using the R factor. The impact of inelastic deformations has to be taken into account in this kind of application. The value of R and  $C_d$  given in the IBC (2000) are estimated by defining the performances of various structural system in prior strong earthquakes, also by technical arguments and customs (NEHRP, 2000). Overstrength, ductility, and energy dissipation through the soil foundation system are explained by the R coefficient (NEHRP, 2000). The selection of R for structural earthquake design has been the subject of several research.

Miranda (1994) provided different approaches to the R coefficient, also known as the strength reduction factor ( $R_\mu$ ). She proposed that  $R_\mu$  is primarily determined by the displacement ductility, structure's natural period and environmental factors.

Volume 12 Issue 11, November 2024

[www.ijser.in](http://www.ijser.in)

Licensed Under Creative Commons Attribution CC BY

Generally speaking, beginning designs for structures follow the comparable static forces specified by building codes. Elastic vibration modes form the basis of the portion of these static forces that is inclusive. Sturdiness and complete safety, which are impossible to achieve during the earthquake with a fair chance of occurrence, are highlighted by current structural design rules. Nonetheless, by using an inelastic energy dissipation system, a number of structural and nonstructural damages can be investigated in order to achieve safety in structural design. The majority of seismic codes assign lower design loads by indicating that structures have a large capacity and overstrength for energy dissipation (ductility  $R_{\mu}$ ).  $R$  combines these characteristics in structural design (Kim et al., 2005). When designing for lateral strength, lateral strength is usually less than what seismic regulations require for structures to remain within the elastic range.

The steel frames'  $\Omega$  and  $R_{\mu}$  were observed by Krawinkler and Osteras (1990) to be in line with UBC's working stress design specifications. Daza (2010) explained the connection between  $R$  and the building's nonlinear static analysis and its essential strength ( $C\Omega$ ), which is based on those mechanisms. Daza claims that codes cannot rationally address the determination of  $R$  because they offer a defined value based on the structural system's experiences. Seismic force reduction factor ( $R$ ) values were found by Shedid et al. (2010) to be approximately 36.0 for matching flanged and end-confined walls and 5.0 for rectangular walls. As to the ASCE-7 standard, the values can be trusted.

The actual  $R$  value for a realistic reinforced concrete (RC) moment-frame building was established by Mondal et al. (2013), and this value was compared with the value recommended for the design in accordance with the Indian standard code. To get close to real  $R$  values for RC moment frames that are practical, they carried out study using Indian norms. For congenital concentric braced frames (CBFs) and buckling-restrained braced frames (BRBFs), Mahmoudi and Zaree (2010) assessed  $R$ . Furthermore, the  $R$  for TADAS frames was proposed by Mahmoudi and Abdi (2012), who

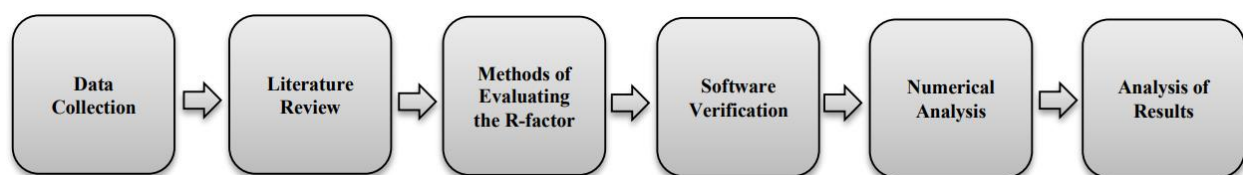
also found that the  $R$  for T-steel moment-resisting frames (SMRFs) has a greater value than SMRFs. Mahmoudi et al. (2013) also looked into the damping and rewarded  $R$  values of frames that have pan friction dampers. Zaree and Mahmoudi (2013) state that  $R$  for BRBFs has high values and that  $R$  is significantly influenced by the number of building height and bracing bays. Zeynalian and Ronagh (2012) conducted research to identify the lightweight knee-braced cold-formed steel constructions' lateral seismic properties.

Applying EBFs to concentrically braced frames, Bosc et al. (2013) anticipated height-wise damage during the breakdown of the EBFs. Galasso et al. (2014) claim that code provisions are not conservative and instead serve as a foundation for improving the calibration of building seismic design codes in the future. A derivation of factors, including  $\Omega$ ,  $R_{\mu}$ , and  $R$ , was created by Izadinia et al. (2012) based on capacity curves obtained using various APA and CPA approaches.  $R$  was assessed by Kappos et al. (2013) for concrete bridges located in Europe.

In the design of seismic construction,  $R$  is a crucial parameter. When estimating structure seismic response, equivalent statistical analysis is commonly used. For the purpose of creating a seismic effect code and non-seismic load condition, the significant factor is generated independently.

## 2. Research Methodology

This study aims to show how the  $R$ -factor is impacted by the outriggers system and how it connects to the value given in the Egyptian code. It shows a flowchart with all the steps required to achieve its objective. First, data is collected from a variety of sources. After that, a review of the relevant literature is done, the various approaches to calculating the  $R$ -factor are examined, and research models are selected. The presentation of the research's findings culminates in a conclusion.



## 3. Concept for Determining Response Modification Factor ( $R$ )

In the past, designing buildings to endure wind and earthquakes was pointless. The majority of structures were built solely to support gravity loads, both dead and live, but lateral loads must now be taken into account. The design requirements for gravity loads and lateral loads are very different. There is less chance of lateral loading. Therefore, it will not be cost-effective to construct a structure to withstand lateral force at the elastic performance level. Specifically, whereas wind loads only account for 1:3 percent of the structure's weight, earthquake loads can reach 30:40 percent. As a result, inelastic performance levels of

collapse prevention and controlled damage should be taken into account.

Response modification factors ( $R$ ), the primary seismic design tool, display the expected degree of inelasticity in structural systems. ASCE 7:2005 defines the  $R$  factor as the "response modification coefficient," IS 1893 (Part 1): (2002) defines it as the "response reduction factor," the Euro code - 8 defines it as the "behavior factor" ( $q$ ), and the Egyptian code ECP-201 (2012) defines it as the "response modification factor ( $R$ -factor)." The  $R$  factor is utilized to lower the design forces that allow us to have an economical structure and reflects a structure's capacity to disperse energy through inelastic performance levels. The component uses a structure's considerable reserve strength and energy-

dissipating ability, known as over strength and ductility, respectively, to explain a structure's nonlinear response (ATC (1995a), Borzi & Elnashai (2000), Rahem et al. (2021)).

Reserve strength and ductility are also taken into consideration by the values allocated to the response modification factor (R) in the US-codes, FEMA [33–35]; UBC1997 (ATC, 1995) [30]. Three factors—ductility, overstrength, and redundancy—that influence the structure's seismic reaction are used by ATC-19 to compute the R-factor.

The main causes of these significant reductions are the over-strength factor ( $\Omega$ ), which takes into account the over-strength introduced in code-designed buildings, and the ductility reduction factor ( $R\mu$ ), which lowers the elastic demand force to the maximum yield strength of the structure. Consequently, the R-factor looks like this:

$$R = R\mu \times \Omega \tag{1}$$

Figures 2 and 3 show the relationship between a structure's base-shear and roof displacement, which may be determined using a nonlinear static analysis.

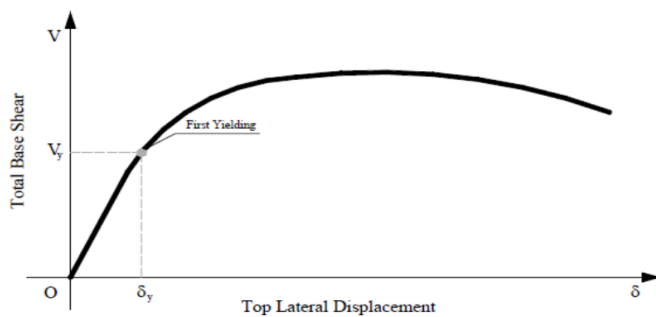


Figure 2: Yield definition as a first yield

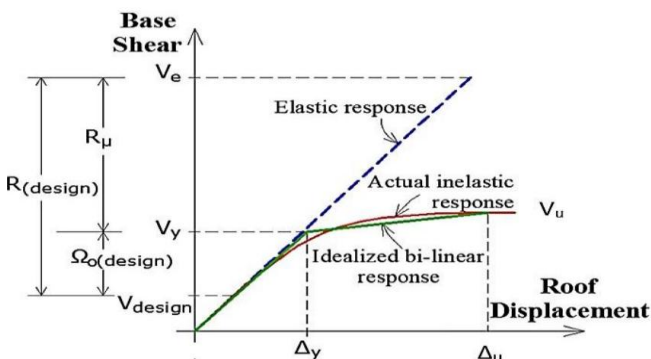


Figure 3: Force displacement response of elastic and inelastic systems

### 3.1 Over Strength Factor $\Omega$

The ratio of actual strength to design level strength is known as the over-strength factor ( $\Omega$ ). It can be stated as follows:

$$\Omega = V_y / V_d \tag{2}$$

where  $V_y$  is the actual strength and  $V_d$  is the design strength

### 3.2 Ductility Reduction Factor $R\mu$

The displacement ductility ratio, or " $\mu$ ," indicates the degree

of inelastic deformation that the structural system experiences when subjected to a specific ground motion or lateral stress. One way to idealize a structure's inelastic characteristics is as follows:

$$\mu = \Delta u / \Delta y \tag{3}$$

where displacement is denoted by  $\mu$ . ductility ratio, yield displacement is denoted by  $\Delta y$ , and ultimate displacement is denoted by  $\Delta u$ . An idealized capacity curve is used to assess yield displacement and yield base shear. Factor that reduces ductility  $R\mu$  depends on the properties of seismic ground motion as well as structural features including ductility, damping, and basic period of vibration ( $T$ ). The following concept, put forward by Newmark & Hall (1982), is applied in this study:

$$R_{\mu} = \sqrt{(2\mu - 1) + 2(T - 0.5) \times (\mu - \sqrt{(2\mu - 1)})} \tag{4}$$

where  $R\mu$  is the ductility reduction factor and  $\mu$  is the displacement ductility.

The idealized pushover curve is used to compute the goal displacement. The FEMA coefficient approach can be used to idealize the pushover curve using the following relation:

$$\Delta u = \delta t = C_0 C_1 C_2 C_3 S_a (T_e^2) / (4\pi^2) g \tag{5}$$

where  $C_0$  is the modification factor that links the roof displacement of the building MDOF system to the spectral displacement of an equivalent SDOF system,  $C_1$  is the modification factor that links expected maximum inelastic displacements to displacements computed for a linear elastic response,  $C_2$  is the modification factor that represents the impact of stiffness degradation, strength deterioration, and pinched hysteretic shape on maximum displacement response, and  $C_3$  is the modification factor that represents increased displacements as a result of dynamic  $P - \Delta$  effects.  $T_e$  is the effective fundamental period of the building in the direction under examination in seconds,  $g$  is the acceleration of gravity, and  $S_a$  is the response spectrum acceleration at the effective fundamental period and damping ratio of the building in the direction under consideration.

## 4. Nonlinear Static Analysis (Pushover Analysis)

The present work determines the global limit states of the RC moment-resistant frame in terms of drift and force level using nonlinear static analysis (pushover analysis). A mathematical model of a building is subjected to the growing forcing function, either in terms of displacements or horizontal forces, which reflect inertial forces along the height of the structure. The analysis is completed when the ultimate limit state or target displacement is reached. The maximum strength and deformation capacity of the building can be ascertained by this kind of investigation. They also assist in locating potential soft and weak tales inside the framework. The loading profile of the first mode shape is used to determine the global limit states using nonlinear static analysis. Modal or Eigenvalue analyses are used to assess the mode forms, the period of structure in each mode, and the modal participation factor. As a preliminary validation tool for the analytical models, this straightforward approach is helpful.

### 5. Finite Element Modeling

It is crucial to precisely simulate the nonlinear behavior of outrigger systems, which are the main structural components of The Iconic Tower that resist lateral forces. It exhibits more complex deformation behavior when subjected to lateral loads. For outrigger systems, it is crucial to concentrate on the nonlinear analysis model.

#### 5.1 Performance-Based Design Methodology

Performance-based engineering produces structures with predictable performance within preset risk and reliability thresholds. Preventing the structure's total collapse is the primary objective. This suggests that while the sub-level, which contains the vital structures, can absorb little damage and still be occupied right away (IO), the top-level can experience a catastrophic collapse (CP). The sub and higher levels are separated by a life safety (LS) level requirement. FEMA's nonlinear methods must be followed in order to define the nonlinear load-deformation relation. Such a curve is shown in Figure 4.

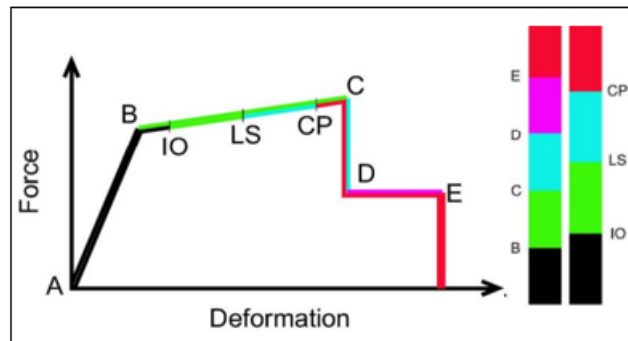


Figure 4: Typical load-deformation relation and target performance levels (ETABS)

FEMA states that the hinge rotation behavior of RC components is described using the five points (A, B, C, D, and E). Three more points—immediate occupancy (IO), life safety (LS), and collapse prevention (CP)—define the hinge's approval standards. Table 1 shows the illustrated damage for concrete frames at different structural performance levels, as provided by ASCE (2017b).

Table 1: Damage for concrete frames at different levels (ASCE, 2017b)

Elements	Immediate Occupancy (IO)	Life Safety (LS)	Collapse Prevention (CP)
Primary Elements	There may be some minor cracking and limited yielding. There is some concrete cover spalling.	extensive beam damage. Shear cracking and cover spalling in ductile columns. Minor spalling in columns that aren't ductile. cracks in joints.	extensive hinge development and cracking in ductile materials. Some non-ductile columns have limited cracking or splice failure. Extreme harm in brief columns.
Secondary Elements	There is also minor spalling in the ductile beams and columns. Flexural fractures in columns and beams. joint shear cracking.	significant hinge development and cracking in ductile materials. Some non-ductile columns have limited cracking or splice failure. Short columns with severe deterioration.	significant spalling in the beams and columns. limited shortening of columns. severe injury to the joints. Some of the reinforcement gave way.
Drift	temporary drift that results in little to no non-structural harm. minimal long-term drift.	It only takes transient drift to result in nonstructural harm. noticeable drift that lasts.	Significant non-structural damage can be caused by transient drift alone. large, ongoing drift.

#### 5.2 Fiber Shell Modeling

It is possible to define the 3D interaction (yield) surface of P-M2-M3 hinges explicitly or automatically using the AISCLRFD equation. H1-1a and H1-1b ( $\Phi=1$ ) ACI 318-02 ( $\Phi=1$ ) for concrete, or FEMA-356 "Equations 4 and 5" for steel. The relationship between M2 and M3 represents the post-yield behaviour, which is interpolated from one or more user-defined P-curves. An energy-equivalent moment-rotation curve is produced during analysis in connection with the interaction-surface yield point and the input P-curve(s).

The postyield behaviour of a beam-column element subjected to combined axial and biaxial-bending circumstances is described by the moment-rotation curve of a P-M2-M3 hinge, which is a monotonic backbone relationship. The envelope of yield points is shown by a P-M2-M3 hinge's 3D interaction surface. Beyond this point, one or more moment-rotation curves must be used to extrapolate performance. because the yield surface is linearly extended by the P-M2-M3 response in three dimensions. While Figure 6 displays the moment and rotation values of a P-M2-M3 moment-rotation curve, which might be derived from fundamental geometric relationships between components projected along the M2 and M3 axes, Figure 5 displays the shell element model for the walls.

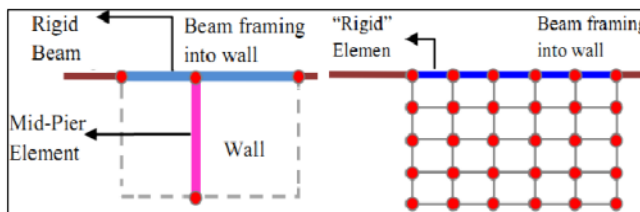


Figure 5: Shell element model for the shear wall

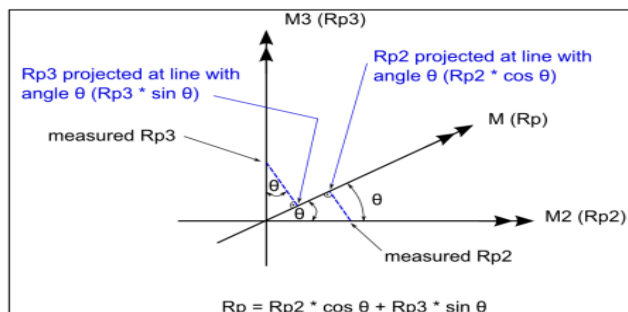


Figure 6: Moment and rotation components

In contrast to the design, uniform ratio, and predetermined arrangement employed in the current investigation, hinge reinforcement might be allocated in a variety of ways. The analysis flow chart is shown in Figure 7.

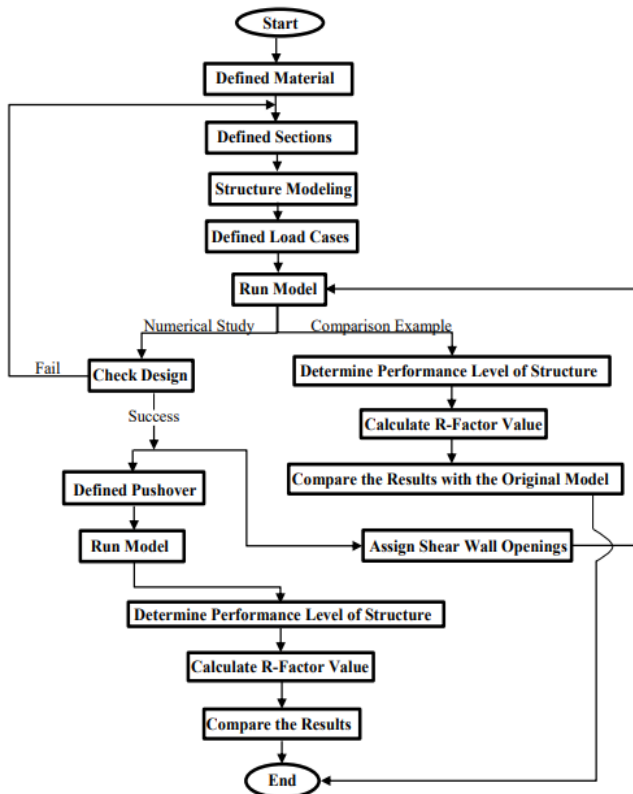


Figure 7: Analysis Flow Chart

## 6. Comparison Example

ETABS software was used to model an eight-story Dual System building that was the subject of a study by Yasser, I., et al.

### 6.1 Model Description

Eight stories There are five bays in each direction of dual-system buildings. The building's overall width is 26.3 meters, and its story height is 3.2 meters. Figure 8 displays the building plan and 3D view. Figure 9 displays the material stress-strain curves for steel and concrete. The shear walls are modeled using two separate modeling techniques (layered and fiber). According to ATC-40 and FEMA 356, nonlinear static pushover analysis is used to do performance-based design on the buildings. With start and end relative distances of 0.05 and 0.95, respectively, plastic hinges are positioned at the points where yielding under seismic stresses is anticipated at both ends of the beams and columns. The walls in the fiber model also have hinges. According to ASCE 41-13, the kind of plastic hinge allotted to beams is M3, which is a single moment rotation type, whereas the type assigned to columns is interacting (P-M2-M3). The walls in the fiber model are (P-M3). The mass source is (Dead Load + Super Dead Load + 0.25 Live Load) in a nonlinear static gravity load case with a zero initial condition and their own weight multiplied by a scale factor of (1), super dead load multiplied by a scale factor of (1), and a live load multiplied by a scale factor of (0.25). Beginning at the conclusion of the nonlinear gravity load case, nonlinear static pushover load cases with a static lateral load pattern in global X-Direction are applied to the structure, with a goal displacement of 4% of the building's overall height.

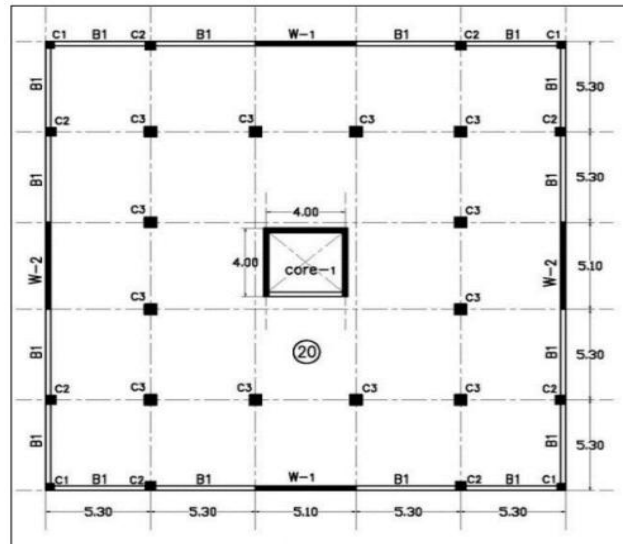


Figure 8 (A): Building plan view

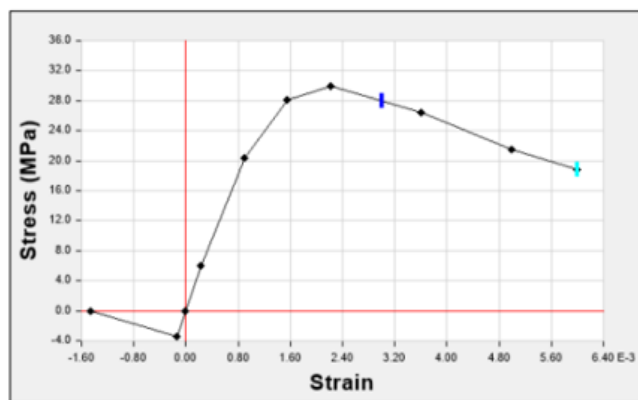


Figure 8 (B): Building 3D-view

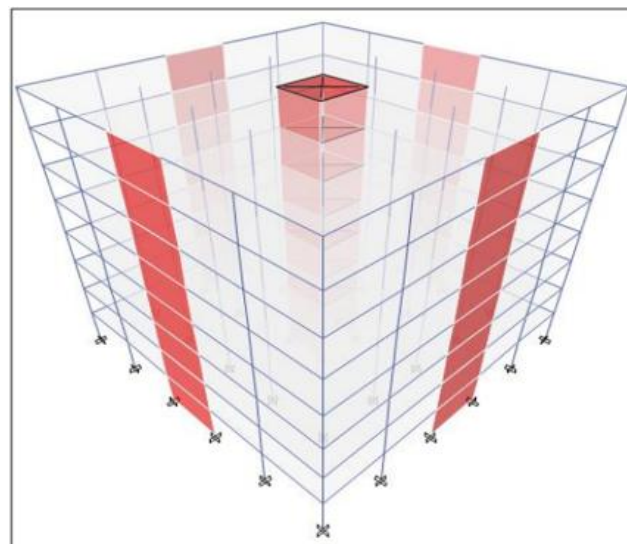


Figure 9 (A): Stress-strain curve for concrete

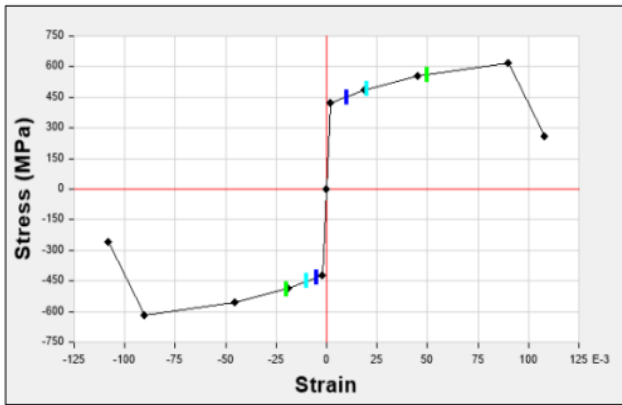


Figure 9 (B): Stress-strain curve for rebar material

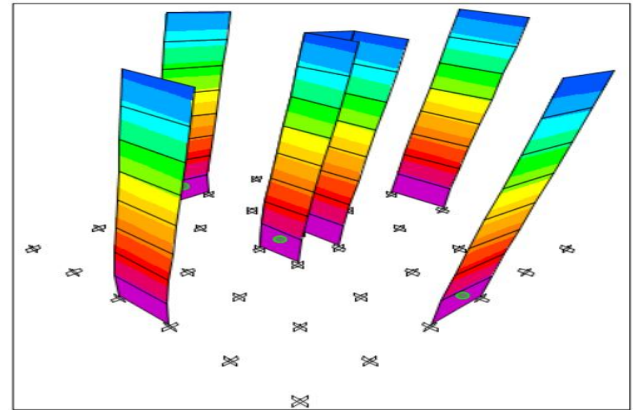


Figure 10 (B): Fiber model displacement

## 6.2 Results and Discussion

- Figure 10 displays the wall displacement, hinge development, and internal stress for fiber and models. The fiber model's internal tensions made it possible to see how hinges formed in walls.
- The fiber model used in this study has been compared to the fiber model pushover curve. It is ideal to use a shear wall fiber model. It allows us to calculate the base shear and top displacement for each level and examine the shear wall's performance levels under lateral loads.
- ETABS v22.2.0 provides precise results that are comparable to the experimental and other software results of other authors and may be appropriate for our investigation. Additionally, by using the perfectible shear wall fiber model, it is possible to evaluate the shear wall's performance levels under lateral loads and calculate the top displacement and base shear for each level.

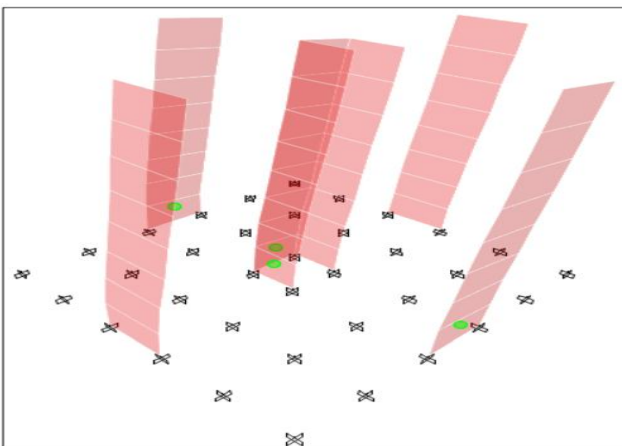


Figure 10 (A): Fiber model hinge formation

## 7. The Iconic Tower Structural System

The Iconic Tower is considered as a high-rise building with concrete foundation at base and sixteen composite columns as the main supporting vertical element along with the concrete core, as shown in Figure 11.A.

The concrete filled tube columns are connected rigidly to the concrete base while for the floor beams are connected rigidly to the composite columns as well.

Outriggers structural system of The Iconic Tower is ensured by supporting floor beams on the composite columns at briefly and concrete core from the other side, however the typical steel beams connections with cores are hinged.

The main transverse seismic resisting system are the cantilever concrete core from inside the tower until the crown level.

To reduce the drift an outrigger system is introduced in floor levels L49 and L73 along with moment resisting frame at radial typically with beams to column connection., as illustrated in Figure 11.B.

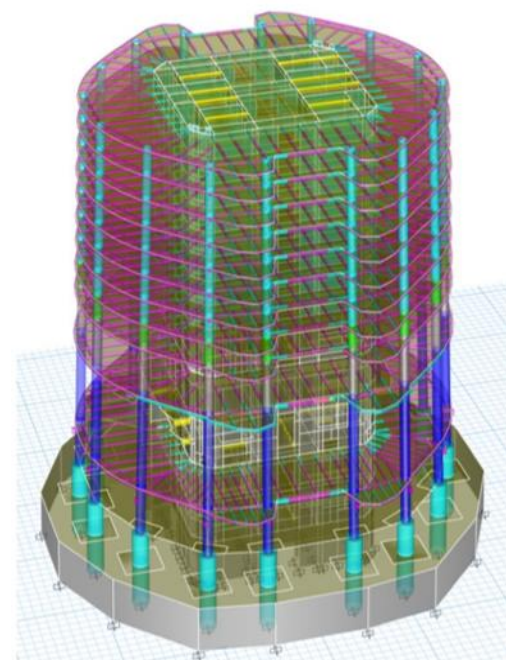


Figure 11 (A): Part of The Iconic Tower structural system near base

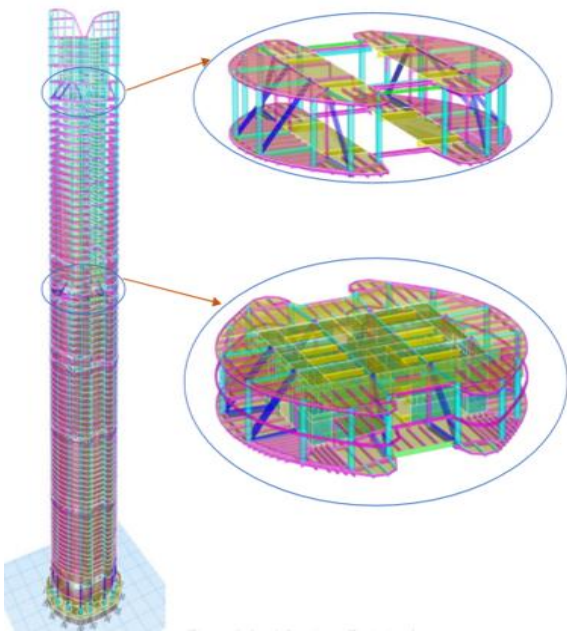


Figure 11 (B): Steel outrigger resisting system

### 7.1 Steel Outrigger

Two Steel outriggers systems are adopted at levels 49 & 73 in order to improve The Iconic Tower strength and overturning by connecting The Iconic Tower concrete core to some of perimeter steel columns as shown on the below figures.

The chosen locations of outrigger are suit architectural and mechanical design since they are selected to be at MEP floors.

The Steel outriggers members have been designed and modeled using ETABS as a part of a compiled model containing steel and concrete elements.

As shown on below figures the embedded outrigger members in the concrete core are connected both floor sides in one direction while in the other direction it was not applicable to do that since there is no concrete member in this direction to embed steel member on it. Therefore, the outrigger system in this direction is connected to the orthogonal outrigger system.

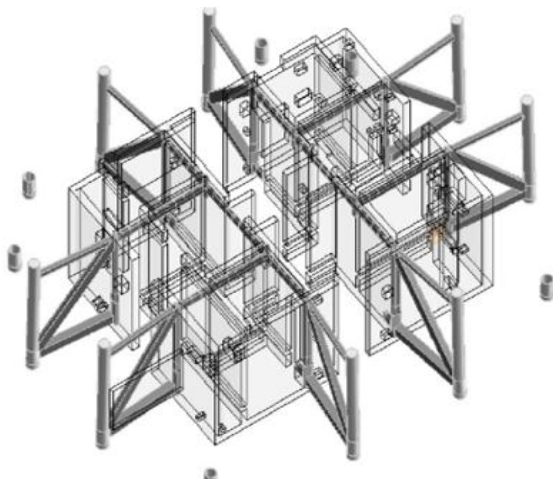


Figure 12 (A): 3D Outrigger system at level 49

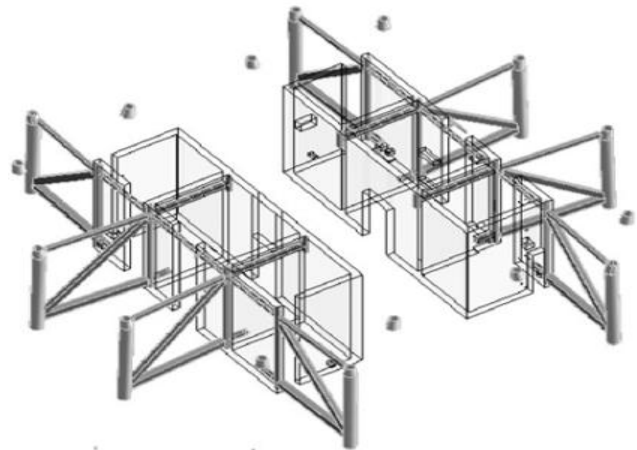


Figure 12 (B): 3D Outrigger system at level 73

### 7.2 Steel Bracing

The statical system of reinforced concrete core is acting as one part from GL to level 50 while it is separated to two parts starting from level 52 to the tower top. The steel bracings are used to connect two parts of RC core together to act as one system.

The steel bracings are used to enhance lateral resisting system of concrete cores and Iconic tower accordingly.

The steel bracings are modeled using ETABS as a part of a compiled model containing steel and concrete elements.

Two steel bracing system are assumed to be used one on each side as shown in Figure 13.A.

Tube sections are used for steel bracings as will explained below.

Steel bracings are connected at both ends rigidly with concrete cores.

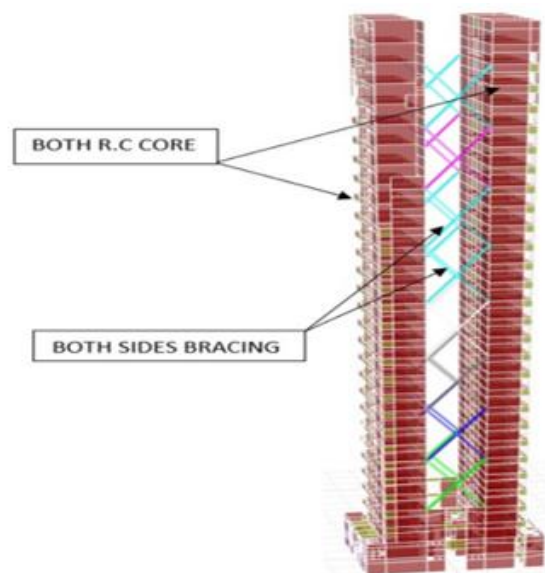


Figure 13 (A): 3D view for analytical model of steel bracing

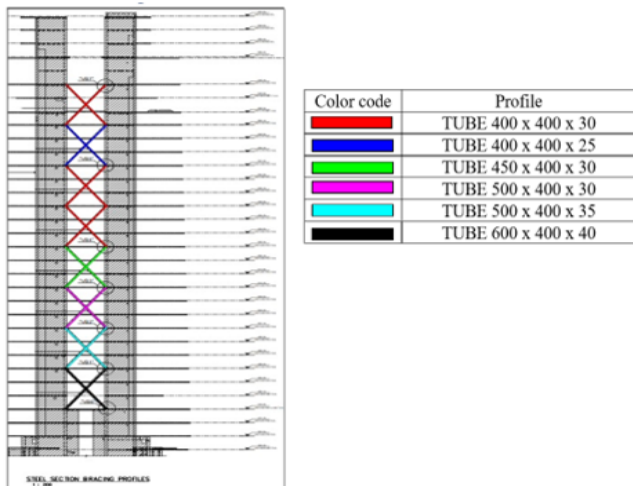


Figure 13 (B): Profiles of steel bracing

## 8. Loads

### Dead Loads

The dead loads in general are different according to Level, however below is brief for the considered dead loads:

- Concrete on metal deck = 310 Kg/m<sup>2</sup> typical for all floors except 348 Kg/m<sup>2</sup> for MEP and heavily loaded floors and other weights for special floors such pool floor.
- Finish screed 100mm = 210 Kg/m<sup>2</sup> typical for all floors, except some floors are granite or glass or no finishes at special floors.
- Raised Floor = 75 Kg/m<sup>2</sup> at offices floors.
- Partitions: at specific floor only, however varies from 250 to 450 kg/m<sup>2</sup>.
- False ceiling = 25 kg/m<sup>2</sup>.
- Fill with foam concrete = varies from 115 to 280 kg/m<sup>2</sup> at specific floors only.
- MEP loads = varies from 70 to 750 Kg/m<sup>2</sup> at specific floors only.
- Planters Load= at four cantilever corners with 700 kg/m<sup>2</sup> soil fill, as required by architect in upper ground floor.
- Curtain walls at edge = 300 kg/m<sup>2</sup> varies according to wall height.

Other loads as Tank loads, Pool walls, special MEP as shown in the ETABS model per floor.

### Live Loads

The live loads in general are different according to Level, however below is brief for the considered live loads:

- Live load = varies from 250 to 500 Kg/m<sup>2</sup> according to the usage.
- Scissor lift as per manufacture catalogue and other loads shown in the ETABS model per floor.

### Wind Loads

The Wind loads are in accordance to the Egyptian code of practice No. 201-2013 as follows:

- Basic wind speed = 33m/s (3sec gust).
- Exposure type = A.

### Seismic Loads

The Seismic loads are calculated as per the Egyptian code of practice No. 201-2013.

- Peak ground acceleration = 0.15 g.
- Soil type = B.
- Spectrum Type II.
- Response reduction factor (R) = 5, 3, 1 for superstructure, raft on soil and raft on piles respectively.

### Temperature Variation

The temperature variation considered is +/-20 0C. In case of thermal analysis, specific membrane stiffness modifier shall be reduced in finite element analysis to as per below schedule to account for cracks. Temperature shall be applied for all structural elements including walls and columns.

## 9. Nonlinear Static Pushover Modeling and Analysis Assumptions

### 9.1 Structural Material

The materials used for The Iconic Tower considered as per (ECP 203) and listed below:

Table 2: The material used for The Iconic Tower

Material Name	Material Type	Elasticity Modulus	Poisson Ratio	Modulus of Shear
F <sub>y</sub> =400 MPa	Rebar	2038.902	—	—
F <sub>y</sub> =500 MPa				
Prestressing Steel Tendons	Tendon	2003.748	0.167	171.936
Cube 45	Concrete	300.979		
Cube 60		347.54		
Cube 60-Composite		401.299		
Cube 80				
Cube 80-Composite				
Cube 80 -RC Column				
Structural Steel Q345		Steel	2039.432	0.29
Structural Steel S420				
Structural Steel Q420-60-100mm				
Structural Steel Q420-40-60mm				
Structural Steel Q420-16-40mm				
Structural Steel Q345-60-80mm				
Structural Steel Q345-40-60mm				
Structural Steel Q345-16-40mm				
Steel ASTM A572		2039.023	0.3	784.24

9.2 Gravity Load Case and Mass Source Data

Gravity load case and mass source data for The Iconic Tower are taken as follows:

Table 3: Mass source data and gravity load case for The Iconic Tower

Load Pattern	Multiplier
OW	1
FC	
PARTITIONS	
EM	
CLADDING	
LL MEP	0.5
LL Park/Ret	
LL Res/Hot/Off	0.25

9.3 The Nonlinear Static Pushover Analysis Modeling Assumptions

The nonlinear static pushover analysis modeling as per ECP-203 for The Iconic Tower are taken as follows:

Table 3: Nonlinear static pushover analysis modeling as per ECP-203 for The Iconic Tower

Modeling Assumptions		
Material	Concrete	Assumptions As per Table 2
	Steel rebar material	
Loading	Stress-Strain relationship	Concrete (Confined according to Mander et al (1988) and unconfined according to ECP-203 stress strain relation). Idealized elasto-plastic stress strain curve for reinforcement steel.
	Self-weight of members	Weight per unit volume = 90 KN/m <sup>3</sup> for steel section and 30 KN/m <sup>3</sup> for concrete section
	Mass source	As per Table 3
	Gravity load case	
	Lateral load	Static triangular load pattern as per ECP-203
	Mass distribution	Distributed on marginal beam and slabs
	P-delta effect	Not considered
Modeling	Element modeling	Frame elements for beam and columns with plastic hinges assigned at start and end of members Fiber model for shear wall elements Shell elements for slabs
	Diaphragm action	Semi rigid diaphragm assigned to joints at each floor
	Base boundary condition	Columns and walls are fixed at base
	Analysis Program	ETABS V 22.2.0

10. Results

The linear dynamic and the nonlinear static pushover analysis results, plotting the pushover curves and calculating  $R_u$ ,  $R_s$  and  $R$  factors for The Iconic Tower model constructed as per ECP203.

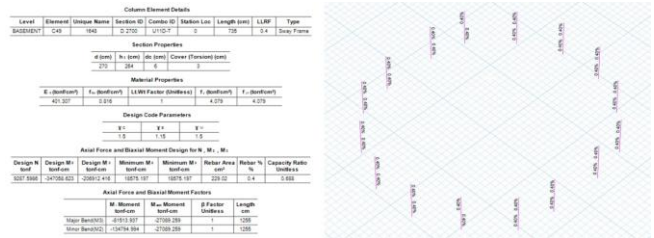


Figure 14: RC Basement column design

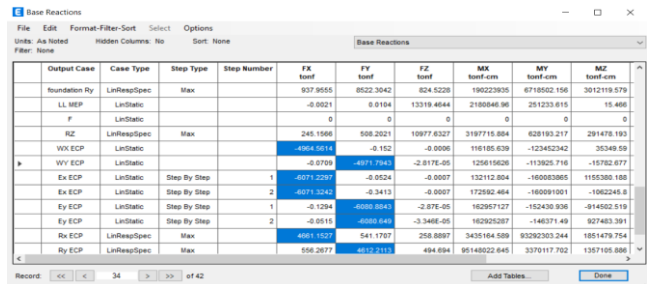


Figure 15: Base shear

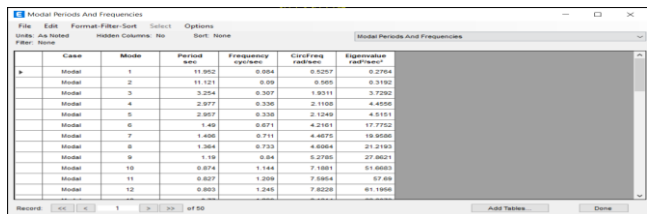


Figure 16: Modal period and frequencies

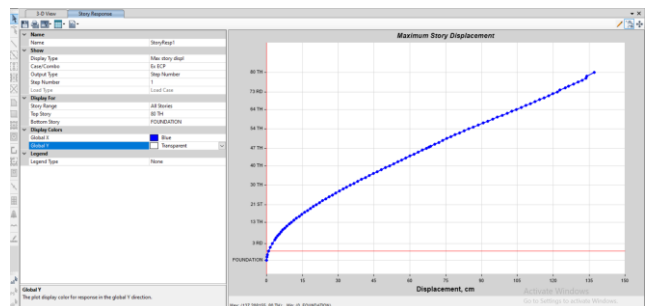


Figure 17: Max story displacement for EX ECP

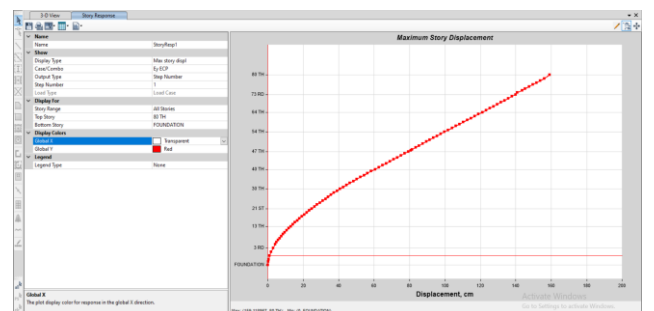


Figure 18: Max story displacement for EY ECP

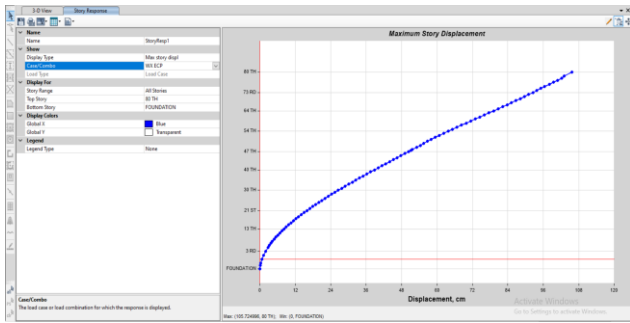


Figure 19: Max story displacement for WX ECP

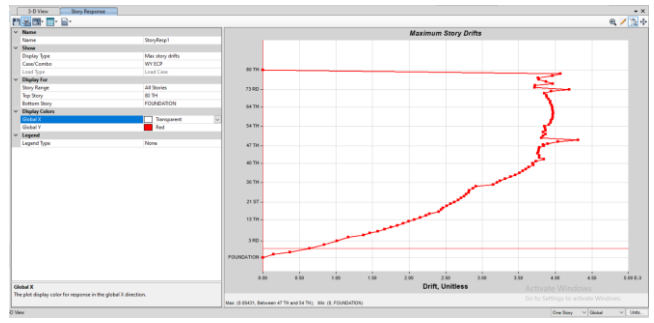


Figure 24: Max story drift for WY ECP

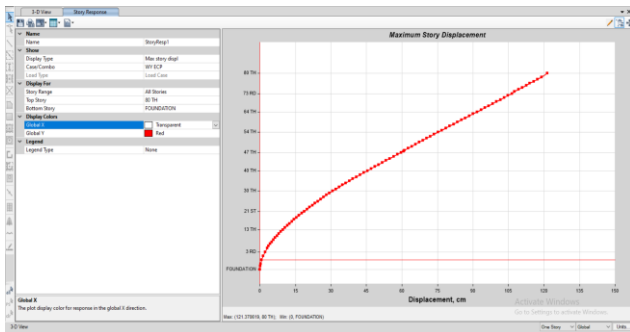


Figure 20: Max story displacement for WY ECP

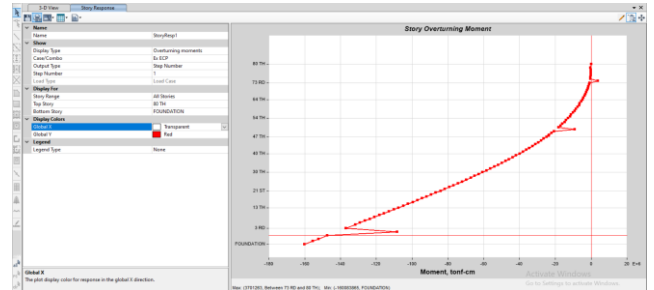


Figure 25: Story overturning moment for EX ECP

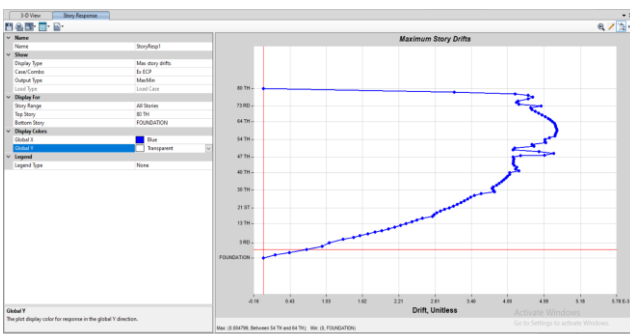


Figure 21: Max story drift for EX ECP

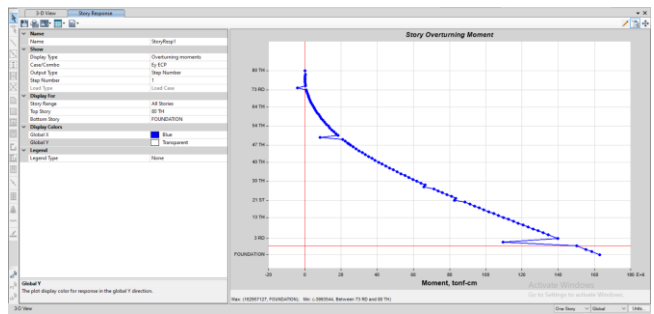


Figure 26: Story overturning moment for EY ECP

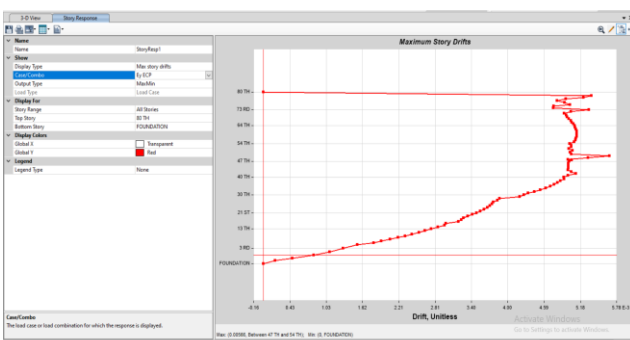


Figure 22: Max story drift for EY ECP

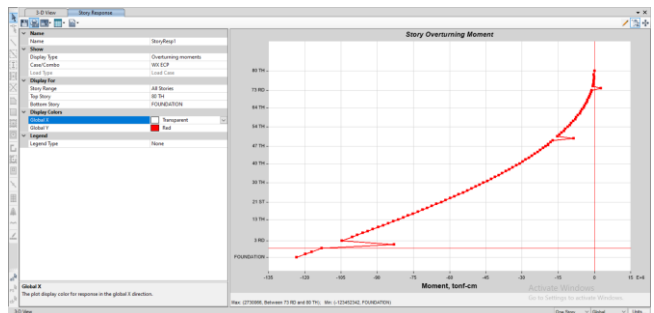


Figure 27: Story overturning moment for WX ECP

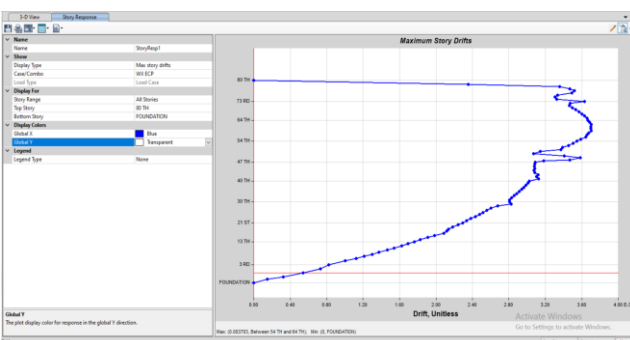


Figure 23: Max story drift for WX ECP

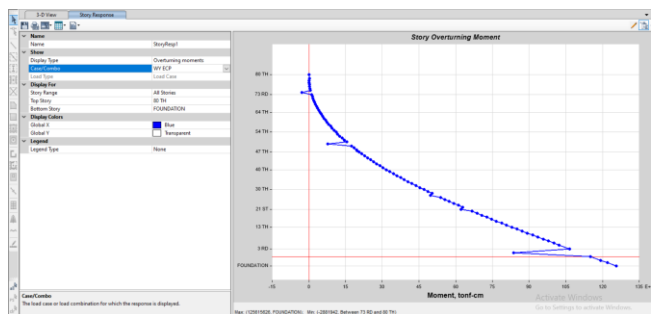


Figure 28: Story overturning moment for WY ECP

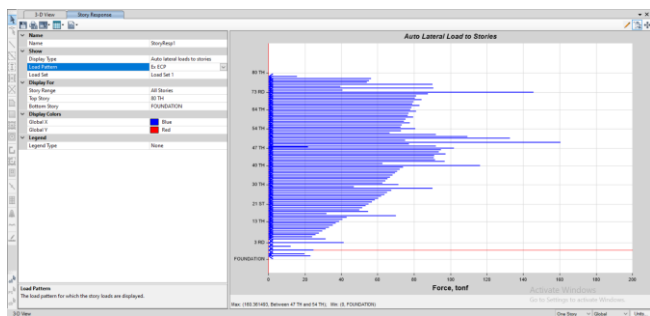


Figure 29: Lateral loads to stories for EX ECP

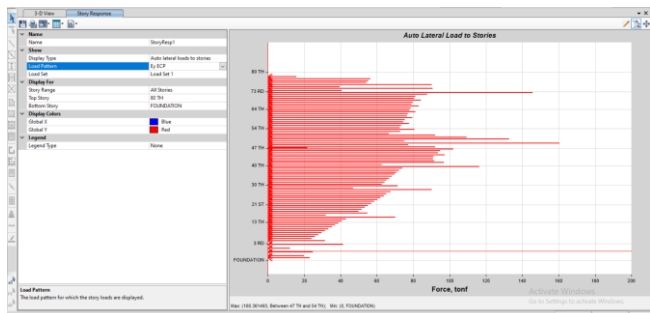


Figure 30: Lateral loads to stories for EY ECP

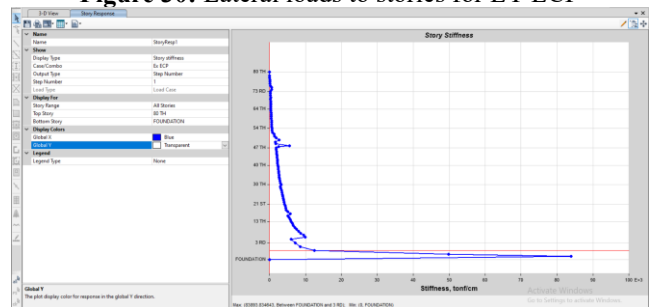


Figure 31: Story stiffness for EX ECP

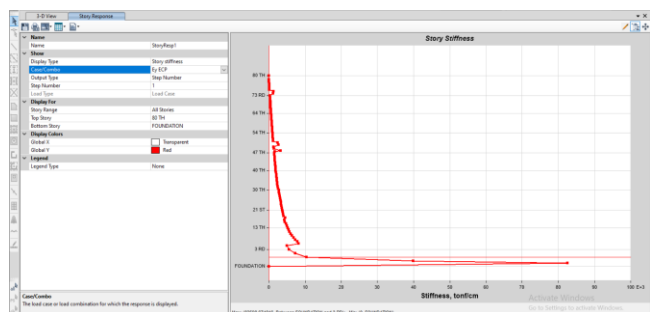


Figure 32: Story stiffness for EY ECP

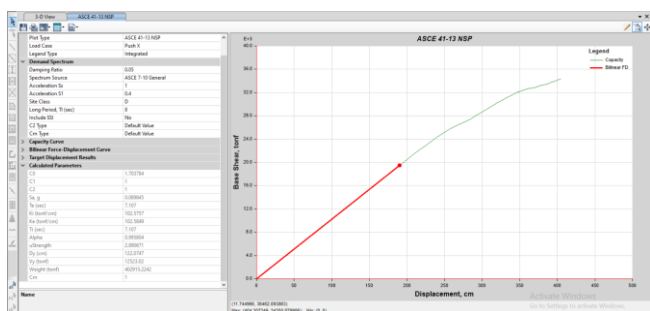


Figure 33: Pushover curve

Table 4: Results for nonlinear static pushover analysis for the iconic tower

Ti (sec)	$\omega$ (1/sec)	$\Delta_{max}$ (cm)	$\Delta_y$ (cm)	$\mu$
7.12	0.14	404.3	122.07	3.31
$R_\mu$	$V_y$ (tonf)	$V_d$ (tonf)	$R_s$	R
3.31	12523.02	6071	2.06	6.82

### 11. Conclusions

A review of previous studies that evaluated the effects of outrigger systems using experimental testing and finite element simulation was conducted. The main conclusions of this study indicate that the outriggers' locations in The Iconic Tower and their existence affect the stiffness and seismic responses of buildings. Also examined were outrigger system structures that were developed in accordance with the Egyptian code of loads, ECP-201 (2012), and verified in accordance with EC8 (2004). The Iconic Tower's seismic response modification factor was determined. An eight-story verified comparative example is provided. Among the most significant results of the work are the following:

- 1) Response modification factor has been highly affected by The Iconic Tower structural system and used code; for The Iconic Tower model results by (ECP 203); the value of  $R_\mu$ ,  $R_s$  and R are 3.312, 2.06 and 6.82 respectively for The Iconic Tower model.
- 2) Structural systems control the distribution and different of the earthquake resisting system elements in addition to the type and distribution of the straining actions acting on these elements, the structural outrigger system is useful and has ability in controlling type and redistribution of straining actions.
- 3) Outrigger system is the economic system for The Iconic Tower and use a smaller number of cores, columns, sections sizes and reinforcement than other systems. R-factor value is reversely proportional to building resistant systems; duplicating on numbers of columns, walls, cores, reinforcement and size of sections and the place of system in building.
- 4) Pushover analysis (POA) has accuracy, efficiency and the design spectrum calculation procedure, so it proposed method to consider as one of the most promising tools for quick seismic assessment for The Iconic Tower.
- 5) Pushover analysis (POA) can predict where plastic hinges may appear and how the structure's strength will decline. POA also detects structural components that might go through crucial stages in the event of an earthquake.
- 6) The results of the response spectrum study used to build The Iconic Tower showed that the immediate occupancy (IO) performance level or pre-yield zone is where the global performance point is located. As a result, there is a sufficient safety margin against collapse, and sufficient displacement and strength are set aside.
- 7) Previous numerical studies have verified the use of finite element software, such as ETABS, to evaluate the nonlinear seismic performance of RC concrete structures. In ultimate and yield base shear, shear and displacement are almost equal.
- 8) The average discrepancy between the results of three different methods for determining the seismic response

modification factor from the pushover curve is less than 10%. In particular, the Park definition for ultimate and yield stages, the ASCE41-13 idealized bilinear curve, and the acceptance criterion limit for hinge deformation

## References

- [1] ECP-201. (2012). Egyptian code for calculating loads and forces in structural work and masonry, Housing and Building National Research Center. Ministry of Housing, Utilities and Urban, Giza, Egypt.
- [2] ETABS Computer Software Package (2021). Computer & Structures Inc. Structural Analysis Programs, CSI Inc., California, United States.
- [3] Yasser, I., Saleh, A., Fayed, M., & Naguib, M. (2018). Response modification factor (R) – The Least understandable in Seismic Codes. 15th International Conference on Structural and Geotechnical Engineering (ICSGE15), 10-13 March 2018, Cairo, Egypt. (Advancements in Construction Techniques).
- [4] Chowdhury, S., A. Rahman, M., J. Islam, M., & K. Das, A. (2012). Effects of Openings in Shear Wall on Seismic Response of Structures. International Journal of Computer Applications, 59(1), 10–13. doi:10.5120/9511-3901.
- [5] Rajesh, M. N., & Prasad, S. K. (2014). Seismic Performance Study on RC Wall Buildings from Pushover Analysis. International Journal of Research in Engineering and Technology, 03(18), 165–171.
- [6] Khatavkar, A. S., Ghadi, A. P., & Barbude, P. A. (2015). Comparative Study of Response Reduction Factor for Reinforced Concrete and Steel Frame. International Journal of Computer Applications: Special Issue International Conference on Quality Upgradation in Engineering, Science and Technology (ICQUEST2015), 12-14.
- [7] BS EN 1998-1. (2005). Eurocode 8: Design of structures for earthquake resistance. General rules, Seismic actions and rules for buildings, London, United Kingdom. doi:10.3403/03244372.
- [8] ATC-19. (1995). Structural Response Modification Factors, Applied Technical Council, California Seismic Safety Commission, Redwood City, California, United States.
- [9] Borzi, B., & Elnashai, A. S. (2000). Refined force reduction factors for seismic design. Engineering Structures, 22(10), 1244–1260. doi:10.1016/S0141-0296(99)00075-9.
- [10] FEMA 273. (1997). NEHRP Guidelines for the seismic Rehabilitation of Buildings. Federal Emergency Management Agency (FEMA), Washington, United States.
- [11] FEMA 356. (2000). Prestandard and Commentary for the Seismic Rehabilitation of Buildings. Federal Emergency Management Agency (FEMA), Washington, United States.
- [12] FEMA 451. (2006). NEHRP Recommended Provisions for Seismic Regulations for New Buildings and Other Structures and Accompanying Commentary and Maps, Federal Emergency Management Agency (FEMA), Washington, United States.
- [13] Park, R. (1989). Evaluation of ductility of structures and structural assemblages from laboratory testing. Bulletin of the New Zealand Society for Earthquake Engineering, 22(3), 155–166. doi:10.5459/bnzsee.22.3.155-166.
- [14] Mwafy, A. M., & Elnashai, A. S. (2002). Calibration of force reduction factors of RC buildings. Journal of Earthquake Engineering, 6(2), 239–273. doi:10.1080/13632460209350416.
- [15] FEMA 303. (1997). NEHRP Recommended Provisions for Seismic Regulations for New Buildings and Other Structures- Part 2: Commentary. Federal Emergency Management Agency (FEMA), Washington, United States.
- [16] Newmark, N. M., & Hall, W. J. (1982). Earthquake spectra and design. Engineering monographs on earthquake criteria, Structural design, and strong motion records (1st Ed.). Earthquake Engineering Research Institute, Oakland, United States.
- [17] ASCE 41-13. (2014). Seismic Evaluation and Retrofit of Existing Buildings. American Society of Civil Engineers, Reston, United States. doi:10.1061/9780784412855.
- [18] IBC2018. (2018). International building Code 2018. International Code Council, Washington, United States.
- [19] ASCE/SEI 7-16 (2017). Minimum Design Loads for Buildings and Other Structures. American Society of Civil Engineers, Reston, United States. doi:10.1061/9780784414248.
- [20] ATC-40. (1996). Seismic evaluation and retrofit of concrete buildings. Applied technology Council, California Seismic Safety Commission, Redwood city, United States.
- [21] ASCE (2017b). Seismic Evaluation and Retrofit of Existing Buildings. Seismic Evaluation and Retrofit of Existing Buildings. American Society of Civil Engineers, Reston, Virginia.
- [22] ACI 318-02/318R-02. (2002). Building code requirements for structural concrete: (ACI 318-02) and commentary (ACI 318R02). American Concrete Institute, Farmington Hills, United States.